ORIGINAL ARTICLE | Neuroradiology

Distinguishing between low-grade and high-grade brainstem glioma using standard MRI pulse sequences

Nguyen Duy Hung[1,2], Ta Van Lam[1], Do Viet Anh[1,2], Nguyen Thu Minh Chau [1,2], Bui Huyen Trang [1,2], Nguyen Minh Duc[3]

[1]*Department of Radiology, Viet Duc Hospital, Hanoi, Vietnam*

[2] *Department of Radiology, Hanoi Medical University, Hanoi, Vietnam*

[3]*Department of Radiology, Pham Ngoc Thach University of Medicine, Ho Chi Minh City, Vietnam*

SUBMISSION: 06/06/2025 | ACCEPTANCE: 10/02/2026

ABSTRACT

Purpose: This retrospective study employs a quantitative analysis of signal intensities derived from standard MRI pulse sequences to differentiate between low-grade and high-grade brainstem gliomas (BSGs).

Material and Methods: Forty-three patients with histopathologically confirmed BSGs underwent gadolinium-enhanced brain MRI. Quantitative parameters, including mean, median, standard deviation, maximum, minimum, and lesion-to-normal tissue ratios, were extracted from volumes of interest (VOIs) placed on pre- and post-contrast T1-weighted, fluid-attenuated inversion recovery (FLAIR), and apparent diffusion coefficient (ADC) maps. Receiver operating characteristic curve analysis was performed to assess the diagnostic performance of each parameter.

Results: Quantitative analysis of T1-weighted and FLAIR sequences revealed that mean T1 signal intensity (T1_mean), median T1 signal intensity (T1_medi-

KEY WORDS

grading brainstem glioma; conventional MR; diffusion-weighted imaging; quantitative.

CORRESPONDING AUTHOR, GUARANTOR

Nguyen Minh Duc, MD, Department of Radiology, Pham Ngoc Thach University of Medicine, 2 Duong Quang Trung Ward 12 District 10 Ho Chi Minh City, Vietnam
Email: bsnguyenminhduc@pnt.edu.vn

an), and minimum FLAIR signal intensity (FLAIR_min) were significant discriminators between low-grade and high-grade BSGs. Optimal cut-off values, sensitivities, and specificities for these parameters were as follows: 559.5 (87.5%, 65.5%) for T1_mean, 576.5 (78.6%, 69%) for T1_median, and 349 (79.3%, 64.3%) for FLAIR_min. Analysis of the solid tumor component on ADC maps identified minimum ADC (ADCs_min) and the ratio of mean ADC to normal white matter ADC (rADCs_mean) as significant discriminators, with optimal cut-off values, sensitivities, and specificities of 862.5 x 10^{-6} mm^2/s (42.9%, 93.1%) and 1.4785 (92.9%, 48.3%), respectively.

Conclusion: Quantitative signal intensity analysis of conventional MRI sequences, particularly T1-weighted and FLAIR, can effectively differentiate between low-grade and high-grade brainstem gliomas (BSGs). Furthermore, analysis of the solid tumor component on ADC maps provides valuable discriminatory information.

Introduction

In contrast to tentorial gliomas, brainstem gliomas (BSGs) are relatively uncommon, with an incidence of approximately 0.311 per 100,000 individuals. BSGs exhibit a predilection for the pediatric population, accounting for 10-20% of all intracranial tumors in children, with a peak incidence between 5 and 9 years of age. In adults, BSGs are less frequent, comprising only 1-2% of intracranial tumors [1-4]. Histopathological assessment remains the gold standard for differentiating gliomas from other brainstem lesions and for grading tumor aggressiveness. The World Health Organization (WHO) classifies gliomas into four grades, with grades 1 and 2 designated as low-grade and grades 3 and 4 as high-grade [5,6]. However, obtaining tissue for histopathological analysis necessitates invasive procedures, such as biopsy or surgical resection, which carry inherent risks, including a mortality rate of approximately 2.5-3.8% [9-13]. The prognosis and survival outcomes for patients with BSGs vary significantly depending on tumor grade and patient age. In children, high-grade BSGs are associated with a dismal prognosis, with an average survival time of only 9-13 months, whereas low-grade BSGs have an average survival exceeding 5 years [7]. In adults, the disparity is less pronounced, with average survival times of approximately 26 months for low-grade BSGs and 10-13 months for high-grade BSGs [8]. Therefore, it is crucial to develop effective minimally or non-invasive methods for differential diagnosis, which can assist in prognosis and guide the selection of the appropriate treatment approach.

Magnetic resonance imaging (MRI), with its advantageous characteristics of high spatial and tissue resolution, non-invasiveness, and absence of ionizing radiation, has become the preferred imaging modality for the diagnosis, surgical planning, and post-treatment monitoring of BSGs [9]. While conventional MRI sequences have demonstrated value in assessing BSG grade, their diagnostic performance remains limited. Previous studies have reported sensitivity and specificity values of 62.5% and 46.6%, respectively, for diagnosing low-grade BSGs, and 58.3% and 61.7%, respectively, for diagnosing high-grade BSGs [10]. To enhance diagnostic accuracy, advanced MRI techniques, such as diffusion kurtosis imaging (DKI), diffusion tensor imaging (DTI), perfusion-weighted imaging, and magnetic resonance spectroscopy (MRS), have been employed. However, these advanced sequences often prolong acquisition time and require specialized expertise for image processing and interpretation. Quantitative analysis of advanced diffusion metrics has shown promise in differentiating BSG genotypes, with a combined DKI and DTI histogram model achieving an area under the curve (AUC) of 0.931 for predicting isocitrate dehydrogenase (IDH) mutation status [11]. Similarly, MRS and perfusion-weighted imaging have demonstrated high discriminatory value for BSG grading, with the choline/N-acetylaspartate (Cho/NAA) ratio from MRS yielding an AUC of 0.944 and relative cerebral blood flow (rCBF) from perfusion-weighted imaging achieving an AUC of 0.917 [12].

Qualitative analyses of BSGs using standard MRI sequences have demonstrated limited utility in differentiating tumor grade, as these tumors typically exhibit similar signal characteristics, such as hyperintensity on T2-weighted images and hypointensity on T1-weighted images. Furthermore, features such as necrosis, hemorrhage, and brainstem invasion are not reliably distinctive between low-grade and high-grade BSGs. While quantitative analyses of T1-weighted and T2-weighted signal intensities have been explored in tentorial gliomas, their application to BSGs remains limited [13,14]. Quantitative analysis of the apparent diffusion coefficient (ADC) map, derived from diffusion-weighted im-

aging, has gained traction due to its standardized nature and quantitative metrics, such as mean, maximum, minimum, and standard deviation, which provide a more nuanced characterization of tumor heterogeneity [13,14]. Histogram analysis of ADC maps, which assesses the distribution of ADC values within the tumor, has further enhanced the ability to evaluate tumor heterogeneity and infer underlying biological characteristics [15]. However, challenges remain in defining the optimal volume of interest (VOI) for ADC histogram analysis. Encompassing the entire tumor volume may introduce confounding effects from cystic or necrotic regions, while restricting the VOI to the solid tumor component may not fully capture the tumor's heterogeneity [14,16,17].

While these VOI placement strategies have been investigated in tentorial gliomas, their application to BSGs remains unexplored. Therefore, this study aimed to evaluate the utility of quantitative signal intensity analysis, including histogram analysis of ADC maps, in differentiating between low-grade and high-grade BSGs using standard MRI sequences.

Methods

Data collection

This retrospective cross-sectional study was conducted at the Imaging Diagnosis Center of Viet Duc Friendship Hospital. Patient data were collected between January 2021 and January 2025. The study included 43 patients with histopathologically confirmed brainstem gliomas who underwent preoperative 3.0 Tesla MRI of the brain with gadolinium contrast enhancement. Patients with a prior history of biopsy or treatment (radiotherapy, chemotherapy, or tumor resection) were excluded, as were those with MRI images degraded by artifacts or inadequate imaging parameters. This study was conducted in accordance with the Declaration of Helsinki (2013).

Technique

All patients underwent MRI using a 3.0 Tesla scanner (SIGNA Pioneer; GE Healthcare, USA) with gadolinium-based contrast enhancement. A standardized imaging protocol was employed for all examinations, as detailed in Table 1.

Table 1: Parameters of sequences

Parameters Sequences	Plane	TR (msec)	TE (msec)	Slide thickness (mm)	FOV	Matrix
T1-FLAIR	axial, sagittal	2000-2300	20-25	5	240-260	192x320
T2-FLAIR FS	axial	7500-8500	110-120	5	230-240	200x320
T2 TSE	axial, sagittal, coronal	3900-4700	100-105	4	210-220	256x384
T2 GRE	axial	250-360	8-10	4	210-220	256x384
DWI/ADC	axial	4000-4700	75-80	5	230-240	192x192
T1 3D CE +	axial, sagittal	5.3-6.3	2.0-2.5	1	240	240x300

TR: Repetition time; TE: Echo time; FOV: Field of view

T1-FLAIR: T1-weighted fluid-attenuated inversion recovery

T2-FLAIR FS: T2-weighted fluid-attenuated inversion recovery fat-saturated

T2 TSE : T2-weighted turbo spin-echo

*T2 GRE: T2-weighted gradient-echo or T2**

T1 3D CE+: 3D IR-prepped fast SPGR high-resolution T1-weighted ("BRAVO"); CE+: a single dose of intravenous contrast agent injection (Gadolinium-DTPA 1ml/kg, the injection rate of 5 mL/s)

Image analysis

MRI images, stored in DICOM format, were analyzed using the Medical Imaging Interaction Toolkit software (MITK Workbench v2023.12; Division of Medical Image Computing, German Cancer Research Center, Heidelberg, Germany) [18]. An experienced neuroradiologist performed all image analyses.

Lesion characterization was conducted manually based on the following criteria: [16]

- **Whole Tumor:** On T2W and FLAIR images, the whole tumor was defined as the region encompassing all abnormal signal intensity, including edema, solid components (enhancing and non-enhancing), and necrosis, demarcated by normal brain tissue or cerebrospinal fluid.
- **Tumor Core and Edema:** The tumor core, comprising the solid and necrotic portions, was identified as the central area of heterogeneous signal intensity on T2W and FLAIR images, surrounded by vasogenic edema with homogenous high signal intensity. Edema was defined as the region of high signal intensity extending beyond the tumor core. **(Fig. 1A-B)**
- **Enhancing, Necrotic, and Non-Enhancing Solid Components:** On post-contrast T1W images, the enhancing solid component, necrotic areas, and hemorrhagic components were identified. Necrotic areas were defined as central regions without contrast enhancement, surrounded by enhancing solid tumor. Hemorrhagic components were identified by signal increase on pre-contrast T1 images or signal decrease on T2*-weighted gradient-echo (T2* GRE) images. Homogenous cystic areas with cerebrospinal fluid signal characteristics on T2W and FLAIR images were also classified as necrotic. **(Fig. 1C-H)** The non-enhancing solid component was defined as the residual tumor volume after subtracting the enhancing and necrotic components. **(Fig. 1H)**

It is important to note that not all tumors exhibited all of these components (e.g., enhancing component, edema, necrosis).

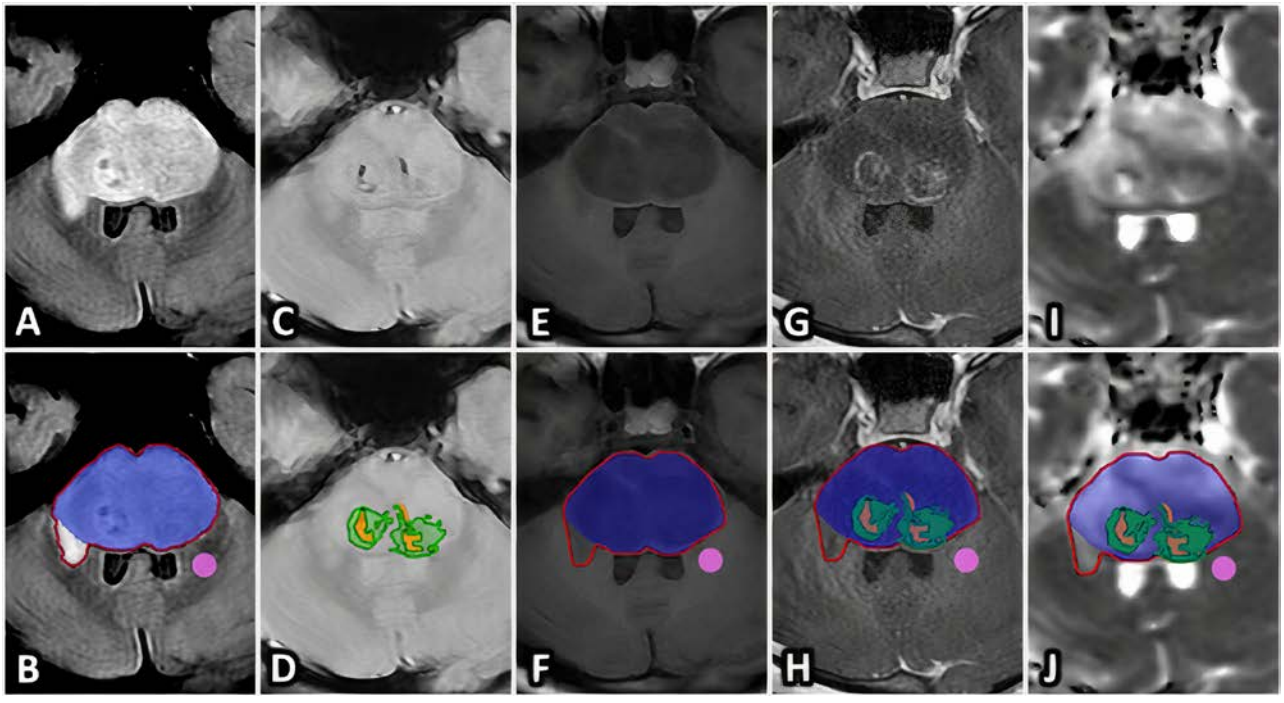

Figure 1. *(A-J) Lesion segmentation and volume of Interest (VOI) definition.* ***A-B.*** *Axial FLAIR images demonstrating the delineation of the tumor core (blue VOI) and peritumoral edema (white VOI) within the whole tumor region (red outline).* ***C-D.*** *Axial T2*-weighted gradient-echo (T2* GRE) images showing the hypointense hemorrhagic component included within the necrotic region (orange VOI).* ***E-F.*** *Axial T1-weighted (T1W) and* ***G-H.*** *axial contrast-enhanced T1-weighted (T1 CE+) images illustrating the identification of the enhancing tumor component (green VOI) and the central necrotic area (orange VOI).* ***I.*** *Axial T1 CE+ image and* ***J.*** *corresponding axial apparent diffusion coefficient (ADC) map showing all segmented tumor components. The pink ROI is placed in normal-appearing white matter to calculate the lesion-to-normal tissue signal intensity ratio.*

From the identified sections, we proceed to place the VOI measuring the entire tumor (red outlined VOI) on the T1 and FLAIR sequences (Fig. 1B, 1F), and to place the VOI of the entire enhancing region of the tumor (green VOI) on the T1-weighted sequence after contrast administration **(Fig. 1H)**. With the ADC map, we place the VOI using two methods: measuring the ADC value of the entire tumor region (VOI 1 - corresponding to the red outlined VOI) and measuring the ADC value of the entire solid part of the tumor (VOI 2 - corresponding to the total of the blue and green VOI). **(Fig. 1J)**. We also proceed to measure an additional ROI in normal white matter to calculate the ratio of the tumor value to that of the white matter. **(Fig. 1B, 1F, 1H, 1J)**.

Histopathological Analysis

Histopathological diagnoses were obtained from either surgical resection or biopsy specimens. All tumors were classified as low-grade or high-grade BSGs according to the 2021 WHO Classification of Tumors of the Central Nervous System.

Statistical Analysis

Statistical analysis was performed using SPSS software (version 20.0; IBM, Armonk, NY, USA). Descriptive statistics for quantitative variables were presented as mean ± standard deviation. The Chi-square test, Fisher's exact test, and Mann-Whitney U test were used to compare categorical and quantitative variables between low-grade and high-grade BSG groups. Receiver operating characteristic (ROC) curve analysis was conducted to determine optimal cut-off values, sensitivity, and specificity for each quantitative parameter in differentiating between the two tumor grades. A p-value < 0.05 was considered statistically significant.

Results

Patient characteristics

This study included 43 patients with BSGs, consisting of 22 males and 21 females. Twenty-five patients were children (<18 years old), and 18 were adults. The cohort comprised 14 patients with low-grade BSGs and 29 with high-grade BSGs. The histopathological diagnoses in the high-grade BSG group were as follows: 10 pilocytic astrocytomas, 1 ganglioglioma, 3 diffuse astrocytomas, 1 anaplastic ependymoma, 7 anaplastic astrocytomas, 20 diffuse midline gliomas, and 1 glioblastoma. There were no statistically significant differences in age or sex distribution between the low-grade and high-grade BSG groups, with p-values of 0.458 and 0.586, respectively.

Quantitative analysis of signal intensities on T1W and FLAIR sequences was performed for the entire tumor volume. Comparisons of these quantitative parameters between the low-grade and high-grade BSG groups are presented in Table 2.

Table 2: Comparison of signal values of the entire tumor on T1W and FLAIR pulse sequence

Parameters	Low grade BSG (Mean±SD)	High grade BSG (Mean±SD)	p (0.05)
T1_mean	615.72 ± 83.00	572.94 ± 118.94	0.049**
T1_median	624.36 ± 85.80	569.31 ± 122.88	0.036**
T1_SD	87.60 ± 40.15	68.81 ± 17.85	0.114**
T1_max	871.79 ± 103.89	836.69 ± 167.23	0.120**
T1_min	322.64 ± 134.42	338.69 ± 99.02	0.938**
r_meanT1	0.7605 ± 0.0927	0.7562 ± 0.0972	0.890*
FLAIR_mean	852.86 ± 120.62	829.92 ± 158.78	0.636*
FLAIR_median	874.42 ± 138.48	823.78 ± 160.98	0.319*
FLAIR_SD	160.98 ± 83.29	97.95 ± 68.20	0.078**
FLAIR_max	1181.29 ± 239.84	1191.00 ± 345.25	0.925*
FLAIR_min	298.50 ± 218.40	444.83 ± 158.75	0.016*
r_meanFLAIR	1.5798 ± 0.1926	1.6677 ± 0.2431	0.243*

** Comparision were performed using the Independent Samples Test*
*** Comparision were performed using the Mann-Whitney U Test*

On T1-weighted (T1W) images, the mean (T1_mean) and median (T1_median) signal intensities of the whole tumor were significantly higher in the low-grade BSG group compared to the high-grade BSG group (p = 0.049 and p = 0.036, respectively). However, the ratio of mean tumor signal intensity to normal white matter signal intensity (r_meanT1) did not differ significantly between the two groups.

On FLAIR images, the minimum signal intensity (FLAIR_min) of the whole tumor was significantly lower in the low-grade BSG group compared to the high-grade BSG group (p = 0.016). Similar to the T1W findings, the ratio of mean tumor signal intensity to normal white matter signal intensity (r_meanFLAIR) did not show a significant difference between the two groups.

Quantitative analysis of signal intensities within the enhancing portion of the tumor on post-contrast T1W images was performed. Comparisons of these quantitative parameters between the low-grade and high-grade BSG groups are presented in Table 3. In the low-grade BSG group, 12 of 14 cases (85.7%) demonstrated contrast enhancement, whereas 18 of 29 cases (62.1%) in the high-grade BSG group showed enhancement. However, there were no statistically significant differences in any of the quantitative signal intensity parameters between the two groups.

Table 3: Comparison of signal values of the tumor's entire enhancing portion of on T1W post-contrast

Parameters	Low grade BSG (Mean±SD) N=12	High grade BSG (Mean±SD) N=18	p (0.05)
T1C+_mean	2248.36 ± 274.42	2241.28 ± 125.04	0.982*
T1C+_max	4448.33 ± 573.33	3823.56 ± 297.49	0.347*
T1C+_min	900.08 ± 138.12	1188.94 ± 79.17	0.062*
r_meanT1C+	1.3118 ± 0.0494	1.2047 ± 0.0617	0.222*

** Comparision were performed using the Independent Samples Test*

Quantitative analysis of signal intensities on ADC maps was performed using two different VOI placement methods:

(1) encompassing the entire tumor volume and

(2) encompassing only the solid tumor component, excluding cystic or necrotic areas. Comparisons of these quantitative parameters between the low-grade and high-grade BSGs groups are presented in Table 4.

Table 4: Comparison of the signal value of the tumor on the ADC map followed two methods of VOI placement: the entire tumor and the entire tumor's solid part

Parameters	Low grade BSG (Mean±SD) $x10^{-6}m^2/s$	High grade BSG (Mean±SD) $x10^{-6}m^2/s$	p (0.05)
Entire tumor			
ADCa_mean	1358.14 ± 315.20	1277.86 ± 337.96	0.460*
ADCa_median	1286.40 ± 279.06	1243.85 ± 342.56	0.688*
ADCa_SD	324.54 ± 188.54	296.46 ± 180.06	0.586**
ADCa_max	2629.14 ± 949.66	2425.76 ± 756.94	0.452*
ADCa_min	711.14 ± 159.43	583.59 ± 241.59	0.133**
rADCa_mean	1.9662 ± 0.4024	1.7998 ± 0.4772	0.268*

Table 4: Comparison of the signal value of the tumor on the ADC map followed two methods of VOI placement: the entire tumor and the entire tumor's solid part

Parameters	Low grade BSG (Mean±SD) $x10^{-6}m^2/s$	High grade BSG (Mean±SD) $x10^{-6}m^2/s$	p (0.05)
Entire tumor			
ADCs_mean	1294.16 ± 288.79	1114.02 ± 272.93	0.053*
ADCs_median	1269.91 ± 307.28	1101.20 ± 281.70	0.081*
ADCs_SD	224.39 ± 93.35	183.17 ± 90.14	0.172*
ADCs_max	2157.93 ± 589.32	1816.72 ± 585.16	0.081*
ADCs_min	800.64 ± 191.26	689.41 ± 136.17	0.034*
rADCs_mean	1.8749 ± 0.3746	1.5721 ± 0.3970	0.022*

** Comparision were performed using the Independent Samples Test*
*** Comparision were performed using the Mann-Whitney U Test*

When encompassing the entire tumor volume in the VOI, there were no statistically significant differences in any of the ADC parameters between the low-grade and high-grade BSG groups. However, when restricting the VOI to the solid tumor component, the minimum ADC value (ADCs_min) was significantly higher in the low-grade BSG group compared to the high-grade BSG group (p = 0.034). Similarly, the ratio of mean ADC value within the solid tumor component to the mean ADC value of normal white matter (rADCs_mean) was significantly higher in the low-grade BSG group (p = 0.022).

Table 5 summarizes the diagnostic performance of quantitative MRI parameters that demonstrated significant discriminatory ability between low-grade and high-grade BSGs, based on ROC curve analysis (Figures 2 and 3). On T1W images, the median signal intensity (T1_median) exhibited the highest diagnostic accuracy, with an area under the curve (AUC) of 0.700, an optimal cut-off value of 576.5, a sensitivity of 78.6%, and a specificity of 69%. On FLAIR images, the minimum signal intensity (FLAIR_min) showed good diagnostic performance, with an AUC of 0.719, a cut-off value of 349, a sensitivity of 79.3%, and a specificity of 64.3%. On apparent diffusion coefficient (ADC) maps, using the VOI encompassing the solid tumor component, the ratio of mean ADC value in the solid tumor to that of normal white matter (rADCs_mean) demonstrated the highest diagnostic accuracy, with an AUC of 0.714, a cut-off value of 1.4785, a sensitivity of 92.9%, and a specificity of 48.3%.

Table 5: Significant parameters for distinguishing low-grade and high-grade BSGs on conventional MRI

Parameters	Cut-off	Se (%)	Sp (%)	PPV (%)	NPV (%)	AUC
T1_mean	559.50	87.5	65.5	54.5	90.5	0.687
T1_median	576.5	78.6	69	55.0	87.0	0.700
FLAIR_min*	349.0	79.3	64.3	82.1	60.0	0.719
ADCs_min	862.5	42.9	93.1	75.0	77.1	0.655
rADCs_mean	1.4785	92.9	48.3	46.4	93.3	0.714

** Positive correlation: values exceeding the cut-off point indicate high-grade BSGs, whi values below the cut-off suggest low-grade BSGs.*

Discussion

Quantitative analysis of density on computed tomography (CT) scans, measured in Hounsfield units (HU), is widely employed in both research and clinical practice. The absolute nature of HU values ensures consistency across different CT scanners and manufacturers. In

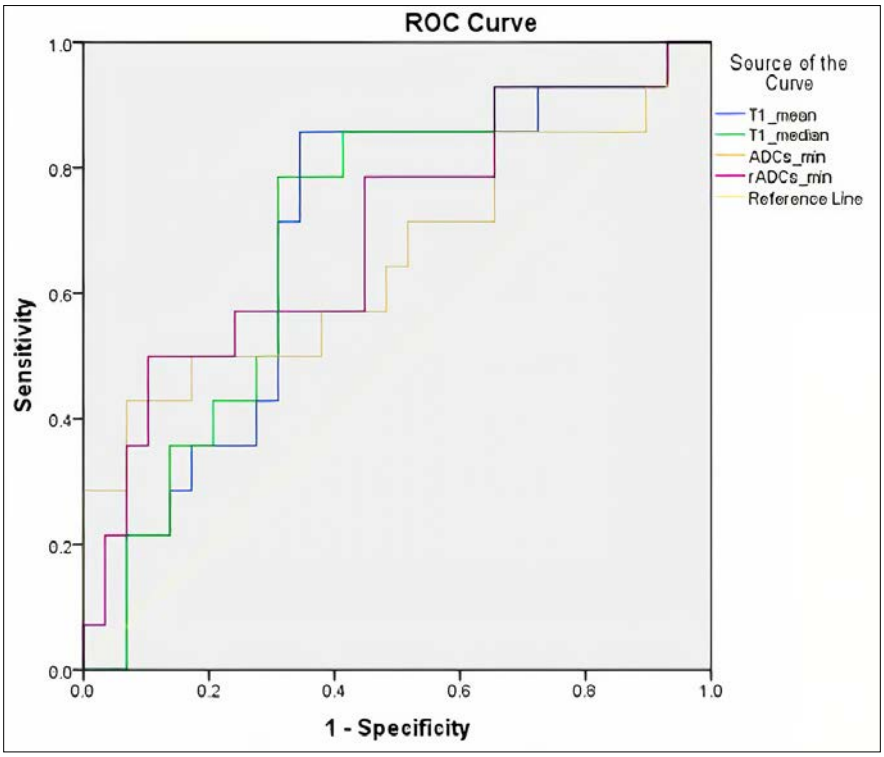

Figure 2: *ROC curve with negative correlation indices significantly distinguishing low-grade BSGs and high-grade BSGs*

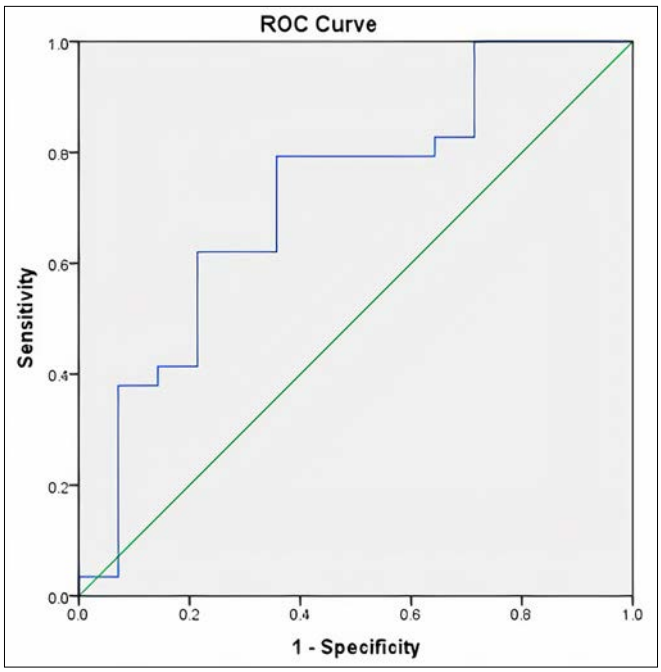

Figure 3: *ROC curve with FLAIR_min index significantly distinguishing low-grade BSGs and high-grade BSGs*

contrast, quantifying signal intensity on MRI is more complex, as signal values are influenced by various factors, including pulse sequence parameters, magnetic field strength, and tissue volume. Consequently, signal intensities can vary depending on the scanner model, manufacturer, and acquisition parameters. Despite these challenges, numerous studies have explored the quantification of MRI signal intensity [19-21]. Standardization techniques are crucial for comparing signal values between different scanners, particularly in large-scale multicenter studies or when compiling datasets for deep learning and artificial intelligence applications. Foltyn et al. [21] demonstrated that standardized signal intensity approaches can effectively minimize inter-scanner variability, even when using identical imaging protocols.

Quantitative MRI studies commonly involve the placement of ROIs or VOIs within tumor lesions, often coupled with the calculation of signal intensity ratios relative to normal brain parenchyma. A fundamental approach entails placing an ROI within a solid tumor region based on radiologist observation. However, this method is susceptible to interobserver variability, poses challenges for automated analysis via artificial intelligence, and may not fully represent the tumor's overall characteristics. An alternative strategy involves delineating a VOI encompassing the entire lesion, thereby capturing the complete spectrum of tumor components. This method facilitates automated processing and reduces observer bias. Nevertheless, the inclusion of diverse tumor components with varying signal properties within a single VOI can influence the overall VOI value.

For instance, necrotic and cystic regions exhibit similar MRI characteristics, including hypointensity on T1W and FLAIR images, hyperintensity on T2W images (similar to cerebrospinal fluid), lack of contrast enhancement, restricted diffusion on DWI, and elevated ADC values due to low cellularity. However, hemorrhagic components within necrotic areas can alter ADC values depending on the stage of blood product degradation [22]. Therefore, a more refined approach involves segmenting distinct tumor components into separate VOIs, preserving the unique characteristics of each region. In this study, we employed two VOI placement strategies, tailored to the specific pulse sequence: (1) a VOI encompassing the entire tumor volume, and (2) VOIs delineating individual tumor components.

While previous studies have rarely employed quantitative analysis of signal intensities on T1W, FLAIR, and post-contrast T1W sequences, our investigation revealed several noteworthy findings. Quantitative assessment of the entire tumor on T1W images demonstrated that both the mean (T1_mean) and median (T1_median) signal intensities were significantly higher in low-grade BSGs compared to high-grade BSGs ($p = 0.049$ and $p = 0.036$, respectively). This highlights the potential value of quantitative signal analysis on T1W images, particularly in cases where qualitative assessment is inconclusive. On FLAIR images, only the FLAIR_min differed significantly between the two groups, being lower in low-grade BSGs ($p = 0.016$). This contrasts with qualitative FLAIR analysis, which did not demonstrate discriminatory ability. Quantitative analysis of the enhancing portion of the tumor on post-contrast T1W images, including assessment of the lesion-to-normal tissue signal intensity ratio, did not reveal any significant differences between low-grade and high-grade BSGs.

Quantitative analysis of DWI, specifically using ADC maps, has been widely employed in differentiating glioma grades, both supratentorially and infratentorially [11,13,14,17,23-28]. In our study, we investigated two methods for ADC quantification: (1) encompassing the entire tumor volume in the VOI, and (2) restricting the VOI to the solid tumor component. When analyzing the entire tumor volume, we did not observe any significant differences in ADC parameters between low-grade and high-grade BSGs, even when incorporating ratios to normal white matter. This contrasts with the findings of Kang et al., [26] who reported that the ADCmin was significantly lower in high-grade gliomas compared to low-grade gliomas ($p < 0.001$).

However, when restricting the VOI to the solid tumor component, we found that the ADCs_min was significantly higher in low-grade BSGs compared to high-grade BSGs ($p = 0.034$), consistent with the observations of Gihr et al. [23]. Furthermore, the rADCs_mean was also significantly higher in low-grade BSGs ($p = 0.022$). This finding differs from the study by Lee et al. [17], which reported no significant difference in the mean ADC ratio between glioma grades. It is important to note that Lee et al. [17] only included the enhancing solid component in their analysis, excluding non-enhancing solid regions. These findings suggest that quantifying ADC parameters within the solid tumor

component may be more valuable than analyzing the entire tumor volume, particularly when assessing BSG grade. Furthermore, incorporating the ratio of tumor ADC to normal white matter ADC can enhance the discriminatory ability of this approach.

This study has several limitations. First, the inclusion of both pediatric and adult patients may have influenced the results, as the epidemiological and imaging characteristics of BSGs can differ significantly between these two groups. Second, the relatively small sample size may limit the generalizability of our findings. Finally, lesion segmentation was performed manually by a single observer, introducing potential subjectivity. While objective segmentation methods using advanced software or artificial intelligence are desirable, they were not feasible in this study due to technical constraints.

Conclusion

Quantitative signal intensity analysis of conventional MRI sequences, particularly T1-weighted and FLAIR, can effectively differentiate between low-grade and high-grade BSGs. Furthermore, analysis of the solid tumor component on ADC maps provides valuable discriminatory information compared to analyzing the whole tumor volume. **R**

Ethical approval

Hanoi Medical University's institutional review board supported this study. This study was conducted according to the ethical standards of the 1964 Declaration of Helsinki and its later amendments.

Informed consent

The requirement for informed consent was obtained.

Availability of data and material

The datasets generated and/or analysed during the current study are not publicly available due to privacy concerns, but are available from the corresponding author on reasonable request.

Conflicts of interest

The authors declare no conflict of interest.

Funding

This research received no external funding.

References

1. Purohit B, Kamli AA, Kollias SS. Imaging of adult brainstem gliomas. European Journal of Radiology. 2015;84(4):709-720. doi:10.1016/j.ejrad.2014.12.025
2. Liu H, Qin X, Zhao L, Zhao G, Wang Y. Epidemiology and Survival of Patients With Brainstem Gliomas: A Population-Based Study Using the SEER Database. Original Research. Frontiers in Oncology. 2021-June-11 2021;11. doi:10.3389/fonc.2021.692097
3. Reyes-Botero G, Mokhtari K, Martin-Duverneuil N, Delattre JY, Laigle-Donadey F. Adult brainstem gliomas. The oncologist. 2012;17(3):388-97. doi:10.1634/theoncologist.2011-0335
4. Ramos A, Hilario A, Lagares A, Salvador E, Perez-Nuñez A, Sepulveda J. Brainstem Gliomas. Seminars in Ultrasound, CT and MRI. 2013/04/01/ 2013;34(2):104-112. doi:doi.org/10.1053/j.sult.2013.01.001
5. Louis DN, Perry A, Reifenberger G, et al. The 2016 World Health Organization Classification of Tumors of the Central Nervous System: a summary. Acta Neuropathologica. 2016/06/01 2016;131(6):803-820. doi:10.1007/s00401-016-1545-1
6. Louis DN, Perry A, Wesseling P, et al. The 2021 WHO Classification of Tumors of the Central Nervous System: a summary. Neuro-oncology. 2021;23(8):1231-1251. doi:10.1093/neuonc/noab106
7. Lam S, Lin Y, Auffinger B, Melkonian S. Analysis of survival in pediatric high-grade brainstem gliomas: A population-based study. Journal of pediatric neurosciences. Jul-Sep 2015;10(3):199-206. doi:10.4103/1817-1745.165656
8. Reithmeier T, Kuzeawu A, Hentschel B, Loeffler M, Trippel M, Nikkhah G. Retrospective analysis of 104 histologically proven adult brainstem gliomas: clinical symptoms, therapeutic approaches and prognostic factors. BMC Cancer. 2014/02/21 2014;14(1):115. doi:10.1186/1471-2407-14-115
9. Sarma A, Heck JM, Ndolo J, Newton A, Pruthi S. Magnetic resonance imaging of the brainstem in chil-

dren, part 1: imaging techniques, embryology, anatomy and review of congenital conditions. Pediatric Radiology. 2021/02/01 2021;51(2):172-188. doi:10.1007/s00247-020-04953-1

10. Rachinger W, Grau S, Holtmannspötter M, Herms J, Tonn J-C, Kreth FW. Serial stereotactic biopsy of brainstem lesions in adults improves diagnostic accuracy compared with MRI only. Journal of Neurology, Neurosurgery & Psychiatry. 2009;80(10):1134-1139. doi:10.1136/jnnp.2009.174250
11. Xiao X, Yang N, Gu G, et al. Diffusion MRI is valuable in brainstem glioma genotyping with quantitative measurements of white matter tracts. European Radiology. 2023/11/06 2023;doi:10.1007/s00330-023-10377-w
12. Tran Dat, Nguyen Duy Hung, Nguyen Ha Khuong, Nguyen Thanh Van Anh, Dong Van He, Nguyen Minh Duc. Diagnostic performance of MRI perfusion and spectroscopy for brainstem glioma grading. European review for medical and pharmacological sciences. Nov 2022;26(21):7938-7948. doi:10.26355/eurrev_202211_30145
13. Gihr GA, Horvath-Rizea D, Hekeler E, et al. Histogram Analysis of Diffusion Weighted Imaging in Low-Grade Gliomas: in vivo Characterization of Tumor Architecture and Corresponding Neuropathology. Original Research. Frontiers in Oncology. 2020-February-25 2020;10doi:10.3389/fonc.2020.00206
14. Liu D, Gao S-X, Liao H-F, Xu J-M, Wen M. A Comparative Study of 2 Different Segmentation Methods of ADC Histogram for Differentiation Genetic Subtypes in Lower-Grade Diffuse Gliomas. BioMed Research International. 2020/09/28 2020;2020:9549361. doi:10.1155/2020/9549361
15. Just N. Improving tumour heterogeneity MRI assessment with histograms. British journal of cancer. Dec 9 2014;111(12):2205-13. doi:10.1038/bjc.2014.512
16. Menze BH, Jakab A, Bauer S, et al. The Multimodal Brain Tumor Image Segmentation Benchmark (BRATS). IEEE Transactions on Medical Imaging. 2015;34(10):1993-2024. doi:10.1109/TMI.2014.2377694
17. Lee J, Choi SH, Kim J-H, Sohn C-H, Lee S, Jeong J. Glioma grading using apparent diffusion coefficient map: application of histogram analysis based on automatic segmentation. NMR in Biomedicine. 2014;27(9):1046-1052. doi:doi.org/10.1002/nbm.3153
18. Goch C, Metzger J, Nolden M. Tutorial: Medical Image Processing with MITK Introduction and new Developments. Springer Berlin Heidelberg; 2017:10-10.
19. Tsien C, Hassan D, Chenevert T, et al. Quantitative measurement of regional signal intensity changes of high grade gliomas following radiotherapy using T1-weighted contrast enhanced MRI imaging. International Journal of Radiation Oncology Biology Physics - INT J RADIAT ONCOL BIOL PHYS. 09/01 2004;60doi:10.1016/j.ijrobp.2004.06.087
20. Sanada T, Yamamoto S, Sakai M, et al. Correlation of T1- to T2-weighted signal intensity ratio with T1- and T2-relaxation time and IDH mutation status in glioma. Scientific Reports. 2022/11/05 2022;12(1):18801. doi:10.1038/s41598-022-23527-9
21. Foltyn-Dumitru M, Schell M, Rastogi A, et al. Impact of signal intensity normalization of MRI on the generalizability of radiomic-based prediction of molecular glioma subtypes. European Radiology. 2024/04/01 2024;34(4):2782-2790. doi:10.1007/s00330-023-10034-2
22. Kang BK, Na DG, Ryoo JW, Byun HS, Roh HG, Pyeun YS. Diffusion-weighted MR imaging of intracerebral hemorrhage. Korean J Radiol. Oct-Dec 2001;2(4):183-91. doi:10.3348/kjr.2001.2.4.183
23. Gihr G, Horvath-Rizea D, Kohlhof-Meinecke P, et al. Diffusion Weighted Imaging in Gliomas: A Histogram-Based Approach for Tumor Characterization. Cancers. Jul 13 2022;14(14)doi:10.3390/cancers14143393
24. Zukotynski KA, Vajapeyam S, Fahey FH, et al. Correlation of (18)F-FDG PET and MRI Apparent Diffusion Coefficient Histogram Metrics with Survival in Diffuse Intrinsic Pontine Glioma: A Report from the Pediatric Brain Tumor Consortium. Journal of nuclear medicine : official publication, Society of Nuclear Medicine. Aug 2017;58(8):1264-1269. doi:10.2967/jnumed.116.185389
25. Server A, Kulle B, Mæhlen J, et al. Quantitative apparent diffusion coefficients in the characterization of brain tumors and associated peritumoral edema. Acta Radiologica. 2009;50(6):682-689. doi:10.1080/02841850902933123
26. Kang Y, Choi SH, Kim Y-J, et al. Gliomas: Histogram

Analysis of Apparent Diffusion Coefficient Maps with Standard- or High-b-Value Diffusion-weighted MR Imaging—Correlation with Tumor Grade. Radiology. 2011;261(3):882-890. doi:10.1148/radiol.11110686

27. Poussaint TY, Vajapeyam S, Ricci KI, et al. Apparent diffusion coefficient histogram metrics correlate with survival in diffuse intrinsic pontine glioma: a report from the Pediatric Brain Tumor Consortium. Neuro-oncology. 2015;18(5):725-734. doi:10.1093/neuonc/nov256
28. Lober RM, Cho YJ, Tang Y, et al. Diffusion-weighted MRI derived apparent diffusion coefficient identifies prognostically distinct subgroups of pediatric diffuse intrinsic pontine glioma. J Neurooncol. Mar 2014;117(1):175-82. doi:10.1007/s11060-014-1375-8

READY - MADE CITATION

Nguyen Duy Hung, Ta Van Lam, Do Viet Anh, Nguyen Thu Minh Chau, Bui Huyen Trang, Nguyen Minh Duc. Distinguishing between low-grade and high-grade brainstem glioma using standard MRI pulse sequences, *Hell J Radiol 2026*; 11(1): 48-59.